

Coronal differential rotation from UVCS/SOHO synoptic observations

S. Mancuso and S. Giordano

*Istituto Nazionale di Astrofisica (INAF), Osservatorio Astronomico di Torino,
Strada Osservatorio 20, 10025 Pino Torinese (To), Italy
(E-mail: mancuso@oato.inaf.it)*

Received: October 21, 2010; Accepted: April 18, 2011

Abstract. Ultraviolet synoptic observations of the O VI 1032 Å spectral line from the UltraViolet Coronagraph Spectrometer (UVCS) telescope aboard the Solar and Heliospheric Observatory (SOHO) have been analyzed in order to establish the rotational characteristics of the solar corona during the minimum and maximum phases of solar cycle 23. By using both autocorrelation and spectral analysis techniques, we determined the solar-cycle dependence of the rotation rate in the middle corona. The UV corona is found to rotate more rapidly and rigidly than the underlying sunspots and photospheric plasma. A systematic and substantial acceleration of the equatorial rotation rate is observed to occur around solar maximum.

Key words: Sun: corona – Sun: rotation – Sun: UV radiation

1. Introduction

The coronal differential rotation remains as yet a poorly understood and debated topic since the determination of rotation rates critically depends upon both the methods applied and the type of data being used. In the corona, the determination of the differential rotation rate is usually obtained indirectly because of the occurrence, at various heliographic latitudes, of localized and bright coronal structures associated with streamers having sufficient stability to reappear, after at least one rotation, at the same limb position. Previous studies of coronal rotation were mainly based on observations obtained in white light (Hansen *et al.*, 1969; Fisher & Sime, 1984; Lewis *et al.* 1999; Lewis & Simnett, 2001), the Fe XIV 5303 Å green line (Sime *et al.*, 1989; Wang *et al.*, 1997; Altrock, 2003), microwaves (Aschwanden *et al.*, 1995), or soft X-rays (Timothy *et al.*, 1975; Weber *et al.*, 1999). Like the underlying photosphere, the corona was observed to rotate faster near the equator and to slow up its rate with latitude toward the poles. Studies of the variation of the coronal differential rotation with time suggest solar-cycle variations in the latitude-dependent rotation linked to the increase in solar activity and the consequent emergence of magnetic flux associated with bipolar regions, with activity speeding up the rotation rate (*e.g.*, Mouradian *et al.*, 2002). On the other hand, from observations of the green solar corona, Rybák (1994) did not find a clear signature of cyclic variation of the

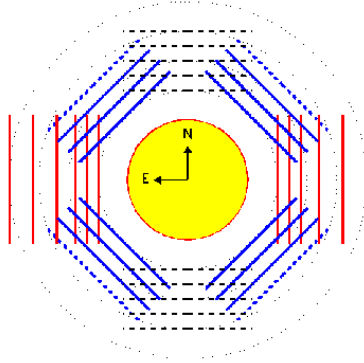


Figure 1. Coronal heights and polar angles observed with the UVCS synoptic program.

rotation over the epoch from 1964 to 1989, while Tlatov (2006), using similar measurements from a wider time interval (1939–2004), claimed that deceleration of the rotational velocity of the corona at low and middle latitudes occurs at activity maxima. Clearly, the long-term variation in the rotation of the solar corona is not well understood as yet.

Compared to other tracers of solar activity, such as sunspots or active regions, coronal spectral lines have the advantage of being detectable over a wide range of heliographic latitudes from the solar equator up to the poles. The extensive database acquired by the UltraViolet Coronagraph Spectrometer (UVCS; Kohl *et al.*, 1995) telescope aboard the Solar and Heliospheric Observatory (SOHO; Domingo *et al.*, 1995) spacecraft extends to an entire solar cycle and contains a wealth of information about the dependence of the coronal rotation rate on time, heliographic latitude, and height. The extended time interval of observation and the high latitude resolution ($\sim 3^\circ$) are both pivotal in recognizing the expected patterns of periodicity due to the coronal differential rotation.

2. Observations and data reduction

The data were collected during regular observations of the coronal O VI 1032 Å spectral line, routinely observed by UVCS/SOHO. The UVCS instrument is an internally and externally occulted coronagraph consisting of two spectrometric channels for the observation of spectral lines in the UV range and a visible light channel for polarimetric measurements of the extended solar corona. The UVCS slit, parallel to a tangent to the solar limb in the plane of the sky, can be moved along the radial direction and is, therefore, able to yield raster observations of the solar corona between 1.4 and $10 R_\odot$ with a field of view of $40'$. In order to cover all possible position angles, the slit can be rotated by 360° about an

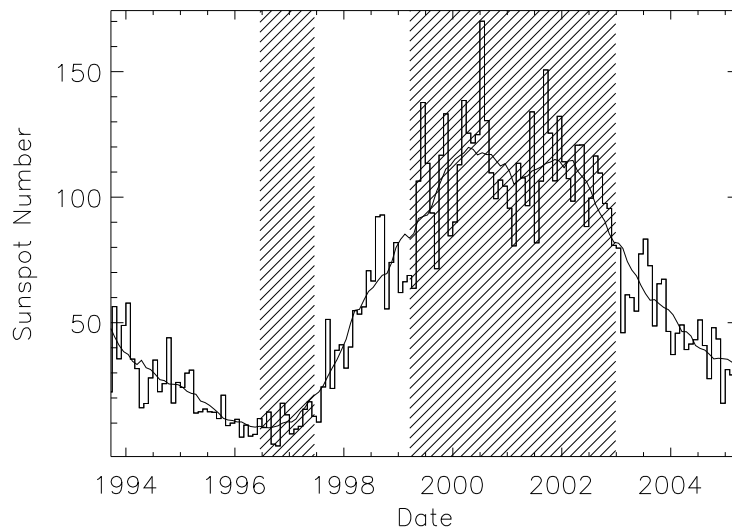


Figure 2. The monthly and monthly-smoothed sunspot numbers from 1994 to 2005. The shaded regions show the two different time intervals that have been used for the study of the coronal rotation at solar minimum and solar maximum. Courtesy of Solar Influences Data Analysis Center (SIDC), Belgium.

axis pointing to the Sun's center. For a complete description of the UVCS instrument, see Kohl *et al.*, (1995). UVCS has been running a counterclockwise daily synoptic observation program which covered the full corona from 1.5 to $3.0 R_{\odot}$ at eight different roll angles separated by an angular step of 45° . On average, the cadence of the data was about one per day, though unevenly spaced in time, with only a small number of gaps due to telemetry problems or special spacecraft maneuvers. An outline of the pointing of the UVCS synoptic observations used for this study is schematically shown in Fig. 1. We only considered data observed with the slit positioned over mid-latitude (45° , 135° , 225° , and 315°) and equatorial regions (90° and 270°). All the O VI intensity data collected in the two time intervals under study (Fig. 2) were used to build up the O VI 1032 \AA intensity synoptic maps shown in Fig. 3. Indeed, both the intensity maps at solar minimum (*upper panel*) and solar maximum (*lower panel*) show a clear modulation which can be readily attributed to the rotation of persistent features through several consecutive rotations. Consequently, the intensity at a fixed location in the synoptic O VI 1032 \AA image gives a suitable time series for an analysis period. We point out that, by visual inspection, it is possible to notice a clear East-West asymmetry in the distribution of the O VI intensity (see

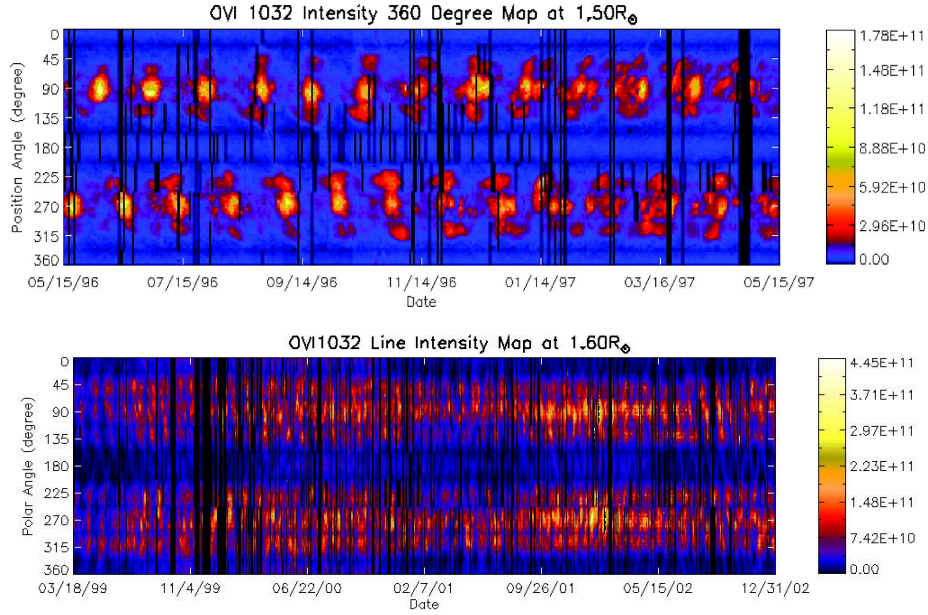


Figure 3. *Upper panel:* An O VI 1032 Å intensity synoptic map in the time interval from mid May 1996 to mid May 1997. The intensities are measured in photons per $\text{cm}^{-2} \text{s}^{-1} \text{sr}^{-1}$. The position angle, measured anti-clockwise from the north pole, increases from top to bottom and covers a full 360° circle at $1.5 R_\odot$. *Lower panel:* An O VI 1032 Å intensity synoptic map at $1.6 R_\odot$ from March 1999 to December 2002.

the upper panel of Fig. 3). This is due to the recurrence of persistent, intense streamer structures associated with active regions that last for more than one rotation and thus appear at the two limbs with a half-rotation delay.

3. Analysis and results

Our analysis is restricted to periodicities on time scales near the 27-day solar rotation period. Two specific methods, the Lomb-Scargle periodogram (LSP; Lomb, 1976; Scargle, 1982) and the autocorrelation function (ACF), have been applied for retrieving the characteristic periods of coronal rotation during solar minimum conditions. In order to double-check the results obtained with the classical ACF method, we also used a *discrete* version of the ACF technique (DACF; Edelson & Krolik, 1988) that is able to detect the level of autocorrelation in unevenly sampled data sets without any interpolation or addition of artificial data points. A number of outliers in the data have been found to be clearly associated with emission from coronal mass ejections (CMEs) that can enhance the observed coronal O VI intensity up to many factors for several tens of minutes

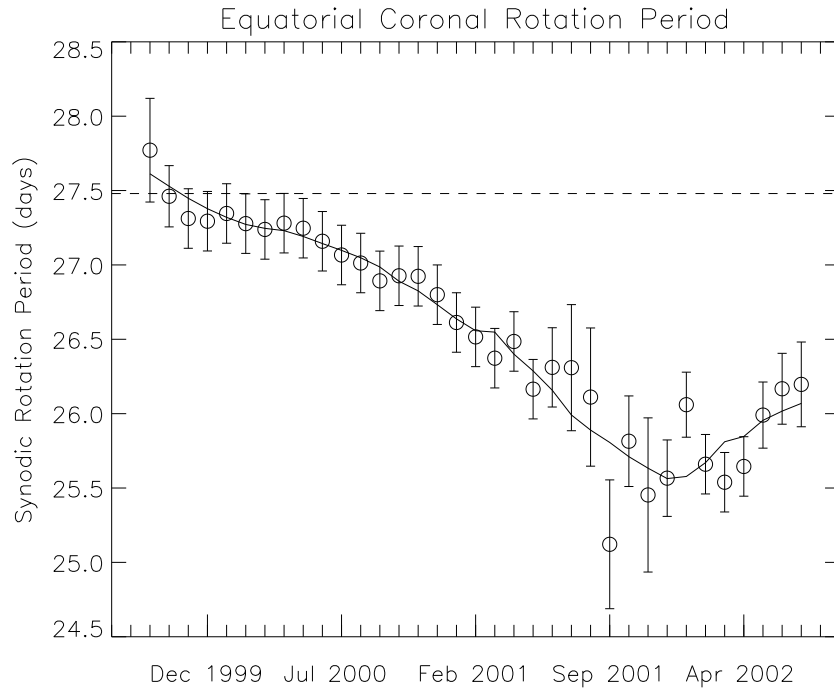


Figure 4. The equatorial coronal rotation period (open circles) as a function of time. The solid line shows a least-squares (Savitzky-Golay) polynomial smoothing filter applied to the data. The dashed line points out the equatorial rotation rate estimated by Giordano & Mancuso (2008) at solar minimum.

(*e.g.*, Mancuso *et al.*, 2002; Mancuso & Avetta, 2008), but the influence of these short lifetime events on the determination of the coronal rotation period was altogether negligible. From the application of both the LSP and D(ACF) analysis to the O VI intensity time series over the two different periods of solar activity, we found that although the estimated equatorial coronal synodic rotation period is initially consistent with the value found by Giordano & Mancuso (2008) around solar minimum (~ 27.5 days), a systematic acceleration occurs in the second half of the year 2000, with the equatorial synodic rotation period settling to an average value of 25.7 days in the time interval extending from August 2001 to April 2002, corresponding to as much as $\sim 7\%$ acceleration of the coronal equatorial rotation rate (Fig. 4). Our results, when compared with the estimate obtained during solar minimum, support the presence of a long-term variation in the rotation of the solar corona, at least around the equatorial region. Mouradian *et al.* (2002), by analyzing the 10.7 cm radio emission flux covering cycles 19–22, established that the active corona rotation rate varies with respect to

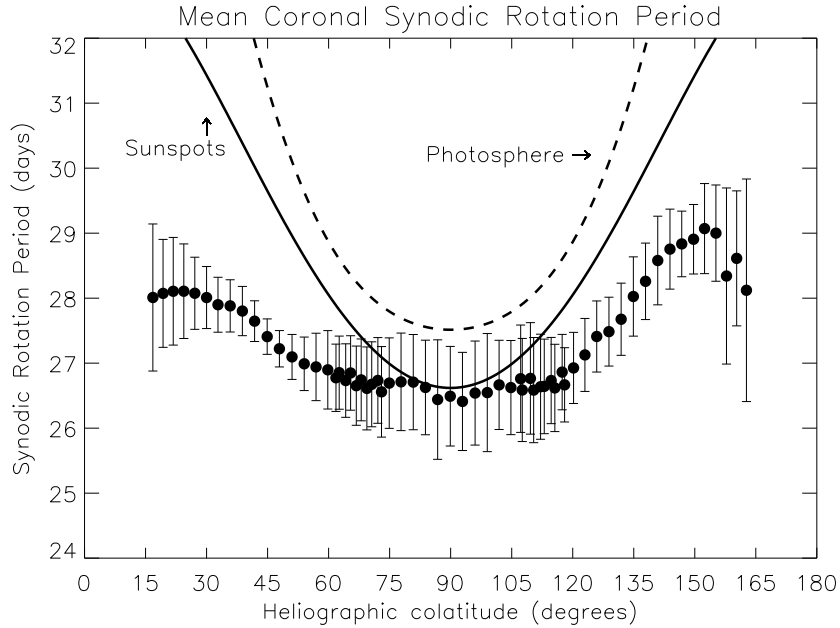


Figure 5. Colatitude dependence of the coronal synodic rotation period in days over the epoch 1999–2002 (filled circles). The dashed and solid lines represent, respectively, analytical approximations to typical differential rotation profiles of the photosphere (Pierce & LoPresto, 1984) and sunspots (Nesme-Ribes *et al.*, 1993) at solar maximum.

the 11 year sunspot cycle and that there is a relationship between the rotation rate and magnetic flux, implying a positive correlation between solar activity and the coronal rotation rate. Since our data do not cover an entire solar cycle, we are not able to confirm or confute the above conclusions.

The coronal rotation rate as a function of heliographic colatitude (Fig. 5) as determined over the full solar maximum time interval confirms the overall rigidity of the corona also during periods of maximum activity with respect to the lower layers of the solar atmosphere. In general, the coronal magnetic structures tend to rotate much faster at all heliographic latitudes, and less differentially, than the underlying small-scale magnetic structures linked to the photospheric plasma. This is consistent with the observation of quasi-rigid rotation of coronal holes (*e.g.*, Timothy *et al.*, 1975). The rotation rate of sunspots is however found to be compatible, at least within a band of $\sim 40^\circ$ around the solar equator, with the one estimated in the middle corona. Finally, the average coronal differential rotation profile at solar maximum is suggestive of a possible North-South asymmetry, as already noticed at solar minimum (Giordano & Mancuso, 2008), with the northern hemisphere appearing to rotate somewhat faster than

the southern hemisphere above $\sim 45^\circ$ from the solar equator. This asymmetry might be tentatively attributed to a viewing effect arising from the inclination of the magnetic field axis with respect to the rotation one (Wang *et al.*, 1997; Mancuso & Garzelli, 2007), although the differences are within the quoted errors at all heliographic latitudes. For more details, see Mancuso & Giordano (2011).

References

- Altrock, R. C.: 2003, *Sol. Phys.* **216**, 343
- Aschwanden, M. J., Lim, J., Gary, D. E., Klimchuk, J. A.: 1995, *Astrophys. J.* **454**, 512
- Domingo, V., Fleck, B., Poland, A. I.: 1995, *Sol. Phys.* **162**, 1
- Edelson, R. A., Krolik, J. H.: 1988, *Astrophys. J.* **333**, 646
- Giordano, S., Mancuso, S.: 2008, *Astrophys. J.* **688**, 656
- Hansen, R. T., Hansen, S. F., Loomis, H. G.: 1969, *Sol. Phys.* **10**, 135
- Kohl, J. L., Esser, R., Gardner, L. D., Habbal, S., Daigneau, P. S., Dennis, E. F., Nystrom, G. U., Panasyuk, A., Raymond, J. C., Smith, P. L., Strachan, L., van Ballegooijen, A. A., Noci, G., Fineschi, S., Romoli, M., Ciaravella, A., Modigliani, A., Huber, M. C. E., Antonucci, E., Benna, C., Giordano, S., Tondello, G., Nicolosi, P., Naletto, G., Pernechele, C., Spadaro, D., Poletto, G., Livi, S., von der Lhe, O., Geiss, J., Timothy, J. G., Gloeckler, G., Allegra, A., Basile, G., Brusa, R., Wood, B., Siegmund, O. H. W., Fowler, W., Fisher, R., Jhabvala, M.: 1995, *Astrophys. J.* **162**, 313
- Lewis, D. J., Simnett, G. M., Brueckner, G. E., Howard, R. A., Lamy, P. L., Schwenn, R.: 1999, *Sol. Phys.* **184**, 297
- Lewis, D. J., Simnett, G. M.: 2001, *Sol. Phys.* **200**, 75
- Lomb, N. R.: 1976, *Astrophys. Space Sci.* **39**, 447
- Mancuso, S., Avetta, D.: 2008, *Astrophys. J.* **677**, 683
- Mancuso, S., Garzelli, M. V.: 2007, *Astron. Astrophys.* **466**, 5
- Mancuso, S., Giordano, S.: 2011, *Astrophys. J.* **729**, 79
- Mancuso, S., Raymond, J. C., Kohl, J., Ko, Y.-K., Uzzo, M., Wu, R.: 2002, *Astron. Astrophys.* **383**, 267
- Mouradian, Z., Bocchia, R., Botton, C.: 2002, *Astron. Astrophys.* **394**, 1103
- Nesme-Ribes, E., Ferreira, E. N., Mein, P.: 1993, *Astron. Astrophys.* **274**, 563
- Pierce, A. K., Lopresto, J. C.: 1984, *Sol. Phys.* **93**, 155
- Rybák, J.: 1994, *Sol. Phys.* **152**, 161
- Scargle, J. D.: 1982, *Astrophys. J.* **263**, 835
- Sime, D. G., Fisher, R. R., Altrock, R. C.: 1989, *Astrophys. J.* **336**, 454
- Timothy, A. F., Krieger, A. S., Vaiana, G. S.: 1975, *Sol. Phys.* **42**, 135
- Tlatov, A. G.: 2006, *Astronomy Reports* **50**, 325
- Wang, Y.-M., Sheeley, N. R., Jr., Hawley, S. H., Kraemer, J. R., Brueckner, G. E., Howard, R. A., Korendyke, C. M., Michels, D. J., Moulton, N. E., Socker, D. G., Schwenn, R.: 1997, *Astrophys. J.* **485**, 419
- Weber, M. A., Acton, L. W., Alexander, D., Kubo, S., Hara, H.: 1999, *Sol. Phys.* **189**, 271